

Evaluating Multiple Instance Learning Strategies for Automated Sebocyte Droplet Counting

Maryam Adelipour¹, Gustavo Carneiro², Jeongkwon Kim^{1*}

¹Department of Chemistry, Chungnam National University, Daejeon, 34134, Republic of Korea

²Centre for Vision, Speech and Signal Processing, University of Surrey, UK

*Correspondence: Jeongkwon Kim jkkim48105@cnu.ac.kr

Abstract

Sebocytes are lipid-secreting cells whose differentiation is marked by the accumulation of intracellular lipid droplets, making their quantification a key readout in sebocyte biology. Manual counting is labor-intensive and subjective, motivating automated solutions. Here, we introduce a simple attention-based multiple instance learning (MIL) framework for sebocyte image analysis. Nile Red-stained sebocyte images were annotated into 14 classes according to droplet counts, expanded via data augmentation to about 50,000 cells. Two models were benchmarked: a baseline multi-layer perceptron (MLP) trained on aggregated patch-level counts, and an attention-based MIL model leveraging ResNet-50 features with instance weighting. Experiments using five-fold cross-validation showed that the baseline MLP achieved more stable performance (mean MAE = 5.6) compared with the attention-based MIL, which was less consistent (mean MAE = 10.7) but occasionally superior in specific folds. These findings indicate that simple bag-level aggregation provides a robust baseline for slide-level droplet counting, while attention-based MIL requires task-aligned pooling and regularization to fully realize its potential in sebocyte image analysis.

Introduction

Sebaceous glands are lipid-secreting skin appendages typically associated with hair follicles, together forming the pilosebaceous unit. Their activity depends on sebocytes, which transition from proliferative basal cells to differentiated cells that accumulate cytoplasmic lipid droplets and ultimately disintegrate through holocrine secretion, releasing sebum. This complex mixture of triglycerides, wax esters, squalene, and cholesterol reinforces the skin barrier and provides antimicrobial and antioxidative protection. The quantity and composition of sebum vary with species and age, and disturbances in sebocyte function are closely associated with dermatological disorders. Excessive secretion and altered lipid fractions are central to acne vulgaris, while sebaceous gland atrophy characterizes several forms of scarring alopecia (1, 2). The human-specific presence of large sebaceous follicles, absent in most other mammals, underscores the importance of studying sebocyte biology directly in human systems. To facilitate such investigations, immortalized sebocyte cell lines have been established as reproducible in vitro models for dissecting sebaceous lipogenesis and evaluating therapeutic strategies (2). A hallmark of sebocyte maturation into fully functional, sebum-secreting cells is the accumulation of intracellular lipid droplets, which represent reliable morphological and functional markers of differentiation (3). Quantitative analysis of these droplets in microscopy images is therefore essential for sebocyte research; yet manual assessment is labor-intensive, subjective, and inconsistent, highlighting the need for automated and robust image analysis approaches. Recent developments in artificial intelligence provide promising solutions to address this need.

Recent developments in artificial intelligence provide promising solutions to address this need. Convolutional neural networks, in particular, have demonstrated remarkable performance in segmentation, classification, and feature extraction, enabling automated processing of large-scale image datasets with accuracy and reproducibility surpassing manual evaluation. These advances highlight the potential of AI to automate microscopy-based diagnostics and experimental workflows, which are traditionally time-consuming and prone to observer variability. Applications span from fundamental biological research, including the study of cell differentiation and intracellular organization, to clinical pathology, where AI-driven image analysis supports disease detection and prognostic assessment using histological slides (4). Moreover, the increasing availability of open-source frameworks and pretrained models has made deep learning more accessible to researchers in cell and developmental biology, thereby lowering the technical barriers for non-specialists and fostering broader adoption (5). This growing ecosystem of tools has paved the way for scalable and reproducible bioimage analysis, yet specific applications—such as the automated quantification of lipid droplets in sebocytes as a proxy for cellular differentiation—remain underexplored, representing an important opportunity for methodological innovation.

In this study, a simple attention-based multiple instance learning (MIL) framework is introduced for sebocyte image analysis. The approach leverages attention mechanisms to identify informative cellular regions and to estimate lipid droplet abundance as a surrogate marker of sebocyte differentiation, without requiring labor-intensive pixel-level annotations. By providing an efficient, scalable, and reproducible solution for droplet quantification, this framework has the potential to advance automated analyses of sebocyte biology and to support both fundamental investigations of sebaceous gland function and translational research into sebocyte-associated skin disorders.

Methodology

Dataset Preparation

Sebocytes were initially expanded in their specific medium (Human Sebocyte Cell Culture Complete Growth Media with serum and antibiotics, Cellprogen). For differentiation, the cells were cultured in Sebomed basal medium (Sigma, USA) supplemented with 1% FBS and 1% penicillin–streptomycin under standard conditions (37 °C, 5% CO₂) for 7 days. Cells were seeded at a density of 30,000 per well into 6-well culture plates (SPL, South Korea). Following differentiation, intracellular lipid droplets were visualized using Nile Red staining according to the manufacturer’s instructions (Abcam, ab228553). Briefly, cells were incubated with Nile Red solution for 30 minutes at 37 °C, washed with PBS, and imaged under a fluorescence microscope (Olympus IX73, Japan) at 20× magnification. The acquired images were saved in JPEG format and compiled into a dataset representing different stages of sebocyte differentiation. This dataset was subsequently used for automated oil droplet quantification and model development. A total of 80 images were acquired over the 7-day culture period, with each image containing on average ~50 sebocytes.

All images were manually annotated using Label Studio. For each image, individual sebocytes were delineated with polygonal masks, and cells were categorized into 14 classes based on the number of visible lipid droplets. Class 1 included cells without droplets, Class 2 represented cells with a single droplet, and subsequent classes incrementally represented higher droplet

counts up to Class 13 (12 droplets). Cells containing more than 12 droplets were assigned to Class 14. To account for heterogeneity in droplet size, a reference droplet size was defined. Very small sub-droplets below this threshold were excluded, while disproportionately large droplets were qualitatively estimated as equivalent to multiple standard droplets, thereby reducing bias between cells with different droplet sizes. After annotation of the 80 original images, data augmentation was applied to increase dataset diversity. Augmentation included brightness adjustment ($0.8\times$ and $1.2\times$ relative to the original images) and Gaussian blurring (kernel size = 3), generating three additional datasets. These augmentations were chosen to reflect realistic variations encountered in microscopy, such as differences in illumination or minor lens adjustments, which can affect image brightness and sharpness. To ensure traceability, all augmented images were saved with unique suffixes appended to the original filenames, and corresponding JSON annotation files were generated with the same suffixes. Individual annotation files were then merged into a single dataset-level JSON file by sequentially appending entries to the list structure of the first file. In total, 80 original images yielded 12,618 annotated sebocytes across 14 classes. The most populated class corresponded to cells containing more than 12 lipid droplets (3,911 cells), while the least represented class was cells with 11 droplets (213 cells). After applying three types of augmentation, the dataset expanded to 320 images comprising approximately 50,000 annotated sebocytes.

Model architecture

Attention-based MIL enables training on weakly labeled data (bags) by learning instance-level attention weights that contribute to bag-level predictions. The seminal work by Ilse et al. (2018) formulated this approach within neural networks, demonstrating superior interpretability and performance across benchmarks, including histopathology dataset (6). The sebocyte classification framework was implemented using a simple attention-based multiple instance learning (MIL) model adapted from the Generalist Pathology Foundation Model (GPFM). In this architecture, each microscopy image is represented as a bag of patch-level feature embeddings, where each instance corresponds to a 512×512 patch processed through a ResNet-50 backbone pretrained on ImageNet. The attention module assigns learnable weights to individual instances, allowing the model to selectively focus on patches most informative for lipid droplet quantification. Aggregated features are subsequently passed through fully connected layers to generate slide-level predictions corresponding to 14 count bins (count₀–count₁₃), reflecting the distribution of droplets per cell. In line with the weakly supervised nature of MIL, this formulation obviates the need for pixel-level annotations and enables learning directly from bag-level labels. To reduce overfitting and improve stability, dropout ($p=0.25$) was applied to the classifier layers, while the feature extractor backbone was frozen during training, ensuring that only the attention and classification components were updated.

Baseline model

To provide a reference framework, a baseline multi-layer perceptron (MLP) model was also implemented. In this setup, aggregated patch-level counts served as direct input features rather than instance-level embeddings. The baseline model consisted of fully connected layers with non-linear activations and dropout regularization, optimized using the same training setup as the MIL model. Unlike the attention-based architecture, which learns to weight informative patches within a bag, the baseline MLP relies solely on bag-level aggregated features, providing a simpler yet informative point of comparison. This baseline allowed us to benchmark the effectiveness of attention-based instance weighting against a conventional bag-level learning strategy.

Training setup

Model training was conducted using five-fold cross-validation to ensure robust evaluation across the dataset. For each fold, slide-level metadata tables (train/validation/test CSVs) were used to define the splits, maintaining balanced representation of the 14 droplet count classes. Training was performed on a single NVIDIA V100 GPU with a batch size of 1 at the bag level, simulating larger effective batch sizes through gradient accumulation. The models were optimized using the Adam optimizer with an initial learning rate of 1×10^{-4} and weight decay of 1×10^{-5} . The loss function was a weighted mean squared error (MSE), where per-class weights were inversely proportional to the mean frequency of each droplet class in the training set, thereby mitigating class imbalance. To improve numerical stability, droplet counts were log-transformed prior to loss computation, and predictions were mapped back to the original scale during evaluation. Early stopping was employed with a patience of five epochs, using mean absolute error (MAE) on the validation set as the monitoring metric. All experiments were repeated across the five folds, and the final performance was reported as the mean and standard deviation across folds.

Evaluation metrics

Model performance was assessed at the slide level using mean squared error (MSE) and mean absolute error (MAE) between predicted and ground-truth droplet count distributions. To improve stability, predictions were first obtained in a log-transformed space and subsequently mapped back to the original scale prior to evaluation. Validation performance was continuously monitored during training, with MAE used as the primary criterion for model selection and early stopping. Final test results were reported as the mean and standard deviation of MAE and MSE across the five cross-validation folds.

Implementation details

All experiments were implemented in PyTorch and executed on a single NVIDIA V100 GPU. Mixed-precision training with automatic loss scaling (AMP) was enabled to improve efficiency. The ResNet-50 backbone used for feature extraction was frozen, and only the attention and classification layers were optimized. Training was performed for up to 120 epochs using the Adam optimizer with a learning rate of 1×10^{-4} and weight decay of 1×10^{-5} . A mini-batch size of 1 was used at the bag level, with gradient accumulation to simulate larger effective batch sizes. Early stopping with a patience of 5 epochs was applied based on validation mean absolute error (MAE) to prevent overfitting.

Results

To increase the size and variability of the dataset, image augmentation was performed. The augmentation parameters were carefully selected so that the overall quality and biological features of the images were not significantly altered. This ensured that key morphological structures, such as lipid droplets within sebocytes, remained clearly visible and biologically interpretable (Figure 1).

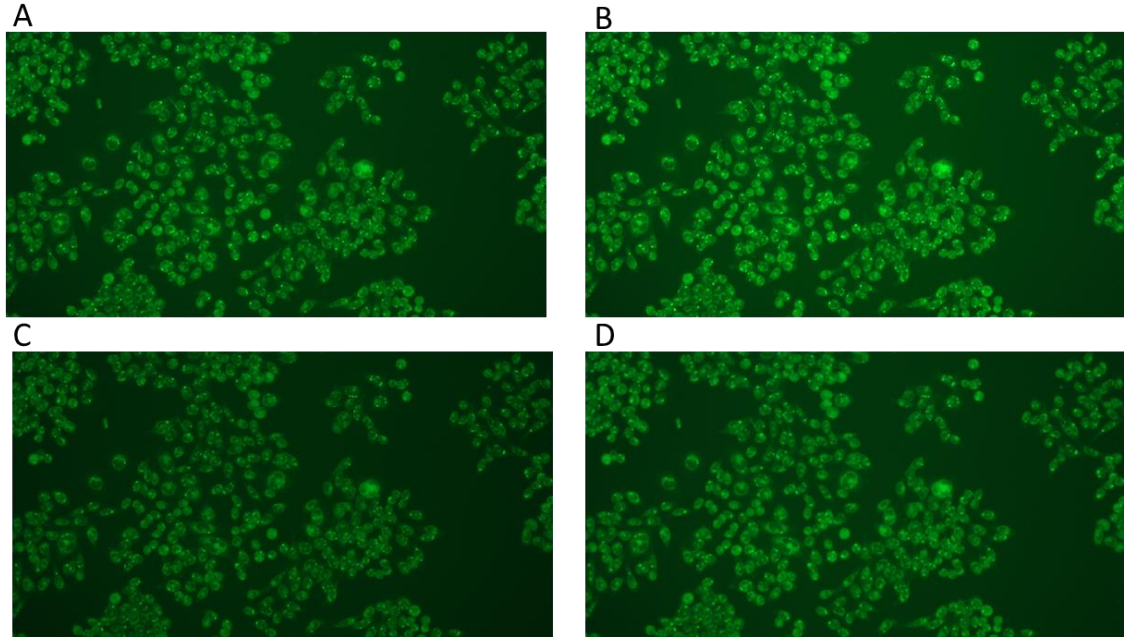


Figure 1. Data augmentation applied to sebocytes stained with Nile Red. A) Original image showing sebocytes with intracellular oil droplets. B) The same image with increased brightness (factor 1.2). C) The same image with reduced brightness (factor 0.8). D) The same image with applied blurriness (kernel size 3).

To establish a reference framework, we implemented a baseline MLP model trained on aggregated patch-level count features. Unlike the attention-based architecture, which learns to assign weights to individual patches within a slide, the baseline model directly operates on bag-level aggregated representations, providing a simpler but informative point of comparison. The baseline model was trained for 200 epochs using three random seeds, and performance was evaluated across five cross-validation folds. As summarized in Table 1, the baseline achieved consistent validation and test performance with mean absolute error (MAE) values around 5.4 (validation) and 5.6 (test), indicating stable generalization across different folds and seeds. These results serve as a benchmark for assessing the added value of the attention-based MIL framework.

Table 1. Validation and test performance (MAE) of the baseline MLP model across folds and seeds.

Seed	Fold	ValMAE	TestMAE	Mean ValMAE	Mean TestMAE
1	0	5.96923	4.826603		
1	1	5.498918	5.844899		
1	2	4.464537	6.729179		
1	3	5.728894	5.510531		
1	4	5.477101	5.172348	5.427736	5.616712
2	0	6.054219	4.85636		
2	1	5.486026	5.957081		
2	2	4.483994	6.686223		
2	3	5.831154	5.625135		
2	4	5.576954	5.315472	5.486469	5.688054
3	0	6.038404	4.878861		

3	1	5.474431	5.807431		
3	2	4.501625	6.74711		
3	3	5.733176	5.579336		
3	4	5.493796	5.267458	5.448286	5.656039
Overall	---	---	---	5.454164	5.653602

To evaluate the effectiveness of the attention-based MIL framework, the adapted GPFM model was trained on aggregated patch-level features. The model was executed with a fixed random seed (Seed = 1) across five cross-validation folds, and an additional run was conducted on fold 1 with Seed = 3 to verify reproducibility. As shown in Table 2, the attention-based model achieved an average validation MAE of 14.41 ± 0.99 and an average test MAE of 10.68 ± 3.46 across folds.

Across all folds, the baseline MLP consistently outperformed the attention-based MIL in terms of mean absolute error, underscoring its stability and reliability under the present data regime. Nevertheless, the attention model occasionally produced competitive results in specific folds (e.g., fold 0 on the test set), suggesting that selective weighting of informative regions can be advantageous when droplet distribution is highly heterogeneous across patches.

Table 2. Validation and test MAE of the attention-based MIL model across folds and seeds.

Seed	Fold	Val MAE	Test MAE
1	0	15.7161	7.9102
1	1	13.1708	16.709
1	2	15.0519	9.1602
1	3	14.0468	9.8206
1	4	14.0468	9.8206
3	1	15.79	7.9979
Summary	---	14.41 ± 0.99	10.68 ± 3.46

Discussion

Across experiments, the attention-based MIL configuration converged in substantially fewer epochs due to early stopping and exhibited higher performance variance across random initializations, whereas the baseline MLP trained on aggregated patch-level counts yielded more stable and, on average, lower MAE on both validation and test sets (Table 1 vs. Table 2). This pattern suggests that, under the present data regime and target formulation, the simpler bag-level model generalizes more reliably. A likely explanation is the interaction between model capacity and the attention pooling mechanism. Attention-based MIL explicitly learns to assign high weight to a small subset of instances to form the bag-level prediction. While this can improve interpretability and performance in slide-level classification, it also increases sensitivity to parameter initialization and promotes “attention concentration,” which has been linked to overfitting and instability in WSI MIL pipelines. Recent studies show that constraining or diversifying attention (e.g., encouraging high-entropy attention or masking top-K instances) can mitigate overfitting and improve robustness across seeds (7). Task structure

is also critical. The present endpoint is multi-output count regression at the bag (slide) level, where signal is distributed across many patches rather than localized to a few discriminative tiles. In such settings, pooling operators that summarize the *distribution* of instance features can be advantageous over sparse attention that concentrates on top instances. Prior work on WSI regression demonstrates that distribution-based pooling can better capture bag statistics for continuous targets, aligning with the empirical advantage observed for the count-aggregated MLP (8). Reviews of WSI aggregation strategies similarly note that simpler or distribution-aware pooling can reduce variance and improve generalization when targets reflect global slide characteristics rather than focal patterns (9). The attention-based backbone adapted from CLAM and related methods is primarily optimized for weakly supervised slide-level classification and subtyping, where identifying a small set of highly informative regions is desirable. Although these models are data-efficient and interpretable for such tasks, their inductive bias may be misaligned with bag-level count regression unless attention is regularized and calibrated for distributed evidence (10).

Overall, these findings indicate that for slide-level droplet counting across cells, a compact bag-level regressor on aggregated counts offers a strong and stable baseline (Table 1), while attention-based MIL requires task-aligned pooling and explicit regularization to close the gap (Table 2). Future work may explore integrating MIL with distribution-aware pooling operators or explicit attention regularization to reduce variance and better capture global droplet statistics, thereby combining the interpretability of attention with the stability of bag-level aggregation.

Ethics Statement

This study does not involve human participants or animal experiments, and no ethical approval was required.

Funding

This study was funded by the National Research Foundation of Korea (RS-2023-00263303 and 2022H1D3A2A01063847).

Acknowledgments / Computing Resources

The authors acknowledge the use of high-performance computing resources provided by KISTI (Korea Institute of Science and Technology Information).

Competing Interests

The authors declare no competing interests.

References

1. Schneider MR. Lipid droplets and associated proteins in sebocytes. *Experimental Cell Research*. 2016;340(2):205-8.
2. Schneider MR, Zouboulis CC. Primary sebocytes and sebaceous gland cell lines for studying sebaceous lipogenesis and sebaceous gland diseases. *Experimental Dermatology*. 2018;27(5):484-8.
3. Dahlhoff M, Fröhlich T, Arnold GJ, Müller U, Leonhardt H, Zouboulis CC, et al. Characterization of the sebocyte lipid droplet proteome reveals novel potential regulators of sebaceous lipogenesis. *Experimental cell research*. 2015;332(1):146-55.

4. Ali M, Benfante V, Basirinia G, Alongi P, Sperandeo A, Quattrocchi A, et al. Applications of artificial intelligence, deep learning, and machine learning to support the analysis of microscopic images of cells and tissues. *Journal of Imaging*. 2025;11(2):59.
5. Hallou A, Yevick HG, Dumitrascu B, Uhlmann V. Deep learning for bioimage analysis in developmental biology. *Development*. 2021;148(18):dev199616.
6. Ilse M, Tomczak J, Welling M, editors. Attention-based deep multiple instance learning. *International conference on machine learning*; 2018: PMLR.
7. Zhang Y, Li H, Sun Y, Zheng S, Zhu C, Yang L, editors. Attention-challenging multiple instance learning for whole slide image classification. *European conference on computer vision*; 2024: Springer.
8. Oner MU, Chen J, Revkov E, James A, Heng SY, Kaya AN, et al. Obtaining spatially resolved tumor purity maps using deep multiple instance learning in a pan-cancer study. *Patterns*. 2022;3(2).
9. Bilal M, Jewsbury R, Wang R, AlGhamdi HM, Asif A, Eastwood M, et al. An aggregation of aggregation methods in computational pathology. *Medical image analysis*. 2023;88:102885.
10. Lu MY, Williamson DF, Chen TY, Chen RJ, Barbieri M, Mahmood F. Data-efficient and weakly supervised computational pathology on whole-slide images. *Nature biomedical engineering*. 2021;5(6):555-70.